Enhanced coagulation with *in situ* manganese dioxide on removal of humic acid in micro-polluted water

Yubin Zeng, Ziyang Zeng and Junlin Wang

ABSTRACT

The morphology and surface characteristics of manganese dioxide (MnO_2) formed *in situ*, which was prepared through the oxidation of $MnSO_4$ using $KMnO_4$, were studied. The effects of factors including the form of MnO_2, dosage, pH, dosing sequence of *in situ* MnO_2 on the enhanced coagulation were systematically evaluated. The results of analysis by the UV_{254} and permanganate index COD_{Mn} methods indicated that humic acid removal increased from 9.2 and 2.5% to 55.0 and 38.9%, when 10 mg/L of the *in situ* MnO_2 was added in the presence of 2 mg/L of polyaluminum sulfate. The studies of orthogonal experiment revealed that coagulation was most affected by the pH, whereas the dosage of *in situ* MnO_2 and slow stirring duration exhibited a weaker effect. At a pH value of 4.0, *in situ* MnO_2 dosage of 10 mg/L, slow stir over 40 min, and the total solids content was 20 mg/L, the humic acid removal by UV_{254} and COD_{Mn} methods reached 71.2 and 61.2%. These results indicated that the presence of *in situ* MnO_2 enhanced the coagulation and removal of humic acid from water.

Key words | enhanced coagulation, humic acid, *in situ* MnO_2, online dosing method

Yubin Zeng (corresponding author)
Junlin Wang
Department of Water Quality Engineering, School of Power and Mechanical Engineering,
Wuhan University,
Wuhan 430072,
China
E-mail: *zengyubin@whu.edu.cn*

Ziyang Zeng
Department of Chemical Engineering and Applied Chemistry,
University of Toronto,
Toronto M5S 3E5,
Canada

INTRODUCTION

Humic acid, which is a main organic constituent, accounts for 60–90% of the total organic content of natural waters (Traversa *et al.* 2014; Wang *et al.* 2014). The functional groups of humic acid, such as the carboxyl group, hydroxyl group, quinone, and ether, can react with various types of cations or organic reactive groups in water, particularly polar organic compounds to form complexes. These reactions can increase the solubility of insoluble toxic compounds in water; therefore, the existence of humic acid is one of the primary factors that create potential safety hazards in water (El-Rehaili & Weber 1987; McKnight & Aiken 1998; Chai *et al.* 2013).

Humic acid treatments can be divided into physical, physico-chemical and biological methods (Brattebø *et al.* 1987; Ghernaout *et al.* 2009; Leodopoulos *et al.* 2012). Fang *et al.* (2008) demonstrated an efficiency of 95.2% for humic acid removal by adsorption onto modified zeolites. Humic acid removal using modified ultrafiltration membranes was investigated and demonstrated that the humic acid removal of regenerated cellulose membranes was very promising (Song 2012). A humic acid degradation rate of 40% was achieved through a biological fluidized bed treatment, which utilized cultivated and domesticated microbes and operated under optimized conditions (such as hydraulic load, pH, temperature, and aeration) (Huang 1999). Fenton's peroxidation was used as an advanced oxidation technique to treat high concentrations of humic acid in simulated wastewater, and the mechanism consists of both oxidation and coagulation simultaneously (Wu *et al.* 2010).

Enhanced coagulation is a method that is based on conventional coagulation. By adjusting the pH and increasing the coagulant dosage, the efficacy of the coagulation effect is enhanced. The development of MnO_2 originates from the use of potassium permanganate for pre-treatment of wastewater. During the reduction of potassium permanganate, *in situ*-state MnO_2 is formed; this compound possesses greater reactivity, specific surface area, and absorption capacity than aged MnO_2 (Liang *et al.* 2005; Fan *et al.* 2010). At present, the use of *in situ* MnO_2 in research is primarily focused on its role as both an oxidant and absorbent; more specifically, the latter use is removal of heavy metals, such as cadmium, strontium, and lead, from water (Xu *et al.* 2013; Wan *et al.* 2014). In contrast, relatively few studies have reported using *in situ* MnO_2 as an enhanced coagulant to remove natural organic matter

doi: 10.2166/wst.2015.226

from waters. This paper reports the enhanced coagulation effect of *in situ*-state MnO_2 formed by reacting potassium permanganate and manganese sulphate, which has value for removal of organic pollutants from water.

METHODS

Reagents and water sources

All the reagents used were analytical grade. The concentration of stock solution $KMnO_4$ and $MnSO_4$ was 4.6 mmol/L and 6.9 mmol/L, respectively. Commercial polyaluminium sulfate (PAS) was purchased from a purification-reagent company in Henan province, China, and used in the experiment as the coagulant. The flocculant polyacrylamide (PAM) used in jar tests were provided from other companies. The raw water from East Lake of Wuhan, China was used in this investigation. The initial concentration of humic acid in micro-polluted water by the UV_{254} and permanganate index COD_{Mn} methods was in the range of 0.20–0.80 and 4 mg/L–20 mg/L, respectively.

Experimental methods

Jar tests: the enhanced coagulation test was conducted in a jar filled with 1 L of micro-polluted lake water, and a programmable jar testing apparatus was used with the following procedure: addition of coagulant PAS following 1 min of rapid mixing at 250 rpm, followed by addition of MnO_2 in different forms, rapid mixing at 250 rpm for 1 min. Then, 1 mg/L of PAM was added to the solution, which was subsequently stirred at 150 rpm for 30 min and settling. After settling for 30 min was completed, the samples (1 cm below) were collected and filtered with 0.45 μm cellulose acetate membrane for measurement of COD_{Mn} and UV_{254}.

The effects of different factors on enhanced coagulation were systematically studied. These tests included the comparison between PAS and PAS + MnO_2, the comparison between *in situ* MnO_2 and commercial MnO_2; the effects of pH of the water, temperature, dosage of *in situ* MnO_2, and ratio of $KMnO_4/MnSO_4$, dosing sequence, dosing methods, and mixing time.

Orthogonal experiments: to obtain the optimal enhanced coagulation parameters, a standard orthogonal array matrix L_9 (3^4) was constructed with four major factors and three levels. The four factors and three levels are as follows: (1) pH: 4, 6, 8; (2) dosage of *in situ* MnO_2: 6, 10, 15 mg/L; (3) slow stirring time: 20, 30, 40 min; (4) particulate concentration: 10, 20, 30 mg/L. Results of humic acid removal were analyzed and optimized statistically to identify significant factors and to evaluate optimal values.

The percentage of humic acid removal (%) by UV_{254} and COD_{Mn} measurements was considered as

$$\text{Removal}\,(\%) = 100 - 100C_t/C_0. \quad (1)$$

where C_0 is the initial concentration of humic acid by UV_{254} and COD_{Mn} methods, and C_t is the concentration of humic acid by UV_{254} and COD_{Mn} methods after completing coagulation.

The Brunauer Emmett Teller (BET) specific surface area of *in situ* MnO_2 was determined using nitrogen adsorption-desorption analysis (Ladavos *et al.* 2012). A total of 0.0443 g of sample was used, with nitrogen gas as the adsorbate, in the adsorption measurement under liquid nitrogen at 77.31 K. The specific surface areas of the samples were determined by applying the BET equation to the data.

The zero point of charge (pH_{ZPC}) of the *in situ* MnO_2 was determined using a Malvern Zetasizer at 25 °C. The same mole ratio of $KMnO_4$ and $MnSO_4$ were added into 100 mL of deionized water. 1 M NaOH and 1 M HCl solution was used to adjust the pH values to 2.0, 3.0, 4.0, 5.0, 6.0, 7.0, 8.0, 9.0 and 10.0. The zeta potential at different pH conditions was measured.

The permanganate index was calculated as the chemical oxygen consumption using potassium permanganate solution as the oxidant, which is denoted as COD_{Mn}, in accordance with the standards (*Standard Methods for the Examination of Water and Wastewater* 1998). The UV_{254} absorbance was defined as the absorbance of some organic matter in water in the presence of ultraviolet light with a wavelength of 254 nm. UV_{254} can reflect the content of natural organic matter such as humic acid, molecules that consists of conjugated double bonds, and aromatic compounds with C = O functional groups.

Instruments

X-ray diffraction (XRD) was performed to confirm the crystal structure and identity using X-ray diffractometer (Rigaku D/MAX-RB, Japan) with Cu Kα radiation in the 2θ ranges of 5–80 ° at a scan rate of 1 °/min. The surface structure of samples was determined using scanning electron microscopy (SEM, JSM-5610LV, Japan). The characterizations of the samples were carried out at their optimal working conditions. A glass pH electrode (PHS-25, China)

was used for pH measurement. The instrument used in BET specific surface area was a Micromeritics (Shanghai) automated ASAP 2020 accelerated specific surface area and porosimetry analyzer. The UV_{254} absorbance was measured using a UV-1600 UV/Vis spectrophotometer.

RESULTS AND DISCUSSION

XRD and SEM

The XRD pattern of the *in situ* MnO_2 is shown in Figure 1. The diffraction peak of the *in situ* MnO_2 is relatively weak and wide, which indicates low crystalline structure. Analyzing the XRD pattern as a whole, only one peak is apparent, which suggests that the purity of the *in situ* MnO_2 was relatively high. Given that the diffraction peak is at $2\theta = 37.17^\circ$, a comparison with powder diffraction patterns indicates that the nature of the manganese dioxide is γ-MnO_2 (Fathy *et al.* 2013).

The SEM image of the *in situ* MnO_2 is shown in Figure 2. It can be observed that the *in situ* MnO_2 particles

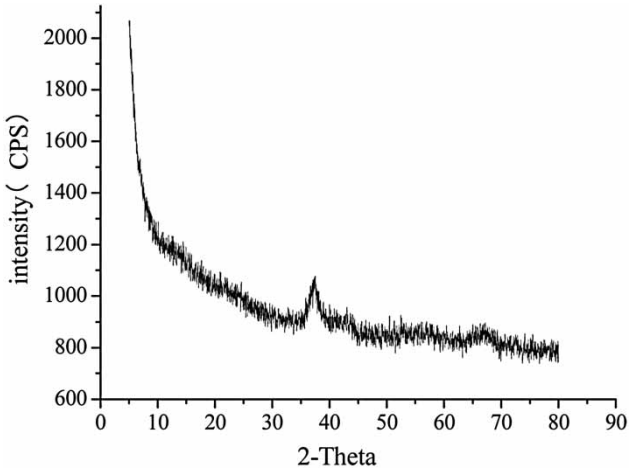

Figure 1 | XRD pattern of the *in situ* MnO_2.

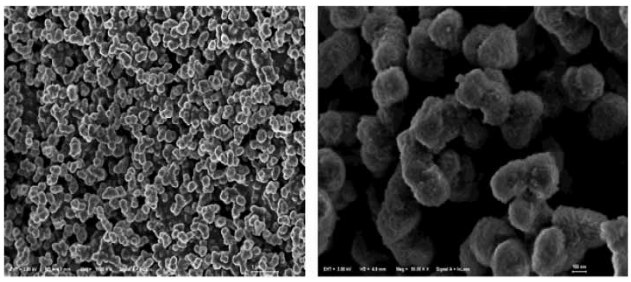

Figure 2 | SEM images of the *in situ* MnO_2.

are amorphous in nature, with a maximum diameter of approximately 120 nm. With an aging time of 30 min, the *in situ* MnO_2 is observed to coagulate into clusters. There is a tendency of increasing aggregation with increasing concentration of the *in situ* MnO_2.

BET specific surface area and pH_{ZPC}

The specific surface area directly governs the contact interfacial area that is available for adsorption. Generally speaking, the adsorption capacity increases with increasing specific surface area. The N_2 adsorption/desorption isotherm of MnO_2 and the fitted curve of the BET equation are shown in Figures 3(a) and 3(b). According to the classification of gas adsorption isotherms, the nitrogen adsorption isotherm of MnO_2 exhibits a steep straight line at low pressures, whereas at high pressures, the adsorption isotherm plateaus at a fixed value. The calculated specific surface area of the MnO_2 is 99.31 m^2/g. The specific surface area of *in situ* MnO_2 is dependent on the preparation method and conditions: Zhang & Ma (2008) used equivalents of $KMnO_4$ to oxidize $MnSO_4$ (small amounts of $NaCO_3$ were added to neutralize the H^+ produced during the reaction), and the specific surface area of the produced *in situ* MnO_2 was 184 m^2/g.

It can be observed from Figure 4 that the zeta potential of *in situ* MnO_2 varies within the tested pH range of 2.0–10.0. The pH_{ZPC} of *in situ* MnO_2 is in the pH range of 2.5–5.0. When the pH of the solution is greater than this value, the surface of the *in situ* MnO_2 is negatively charged, i.e., the zeta potential is negative on the surface of *in situ* MnO_2. Conversely, when the pH is less than the isoelectric point, the zeta potential of the *in situ* MnO_2 is positive (Savaji *et al.* 2014; Kosmulski 2014).

Effect of the form of the manganese dioxide on enhanced coagulation

Figures 5(a) and 5(b) show a comparison between the effects of *in situ* MnO_2 and commercial MnO_2 on the efficiency of enhanced coagulation. It was observed that with increasing coagulant dosage, both UV_{254} removal and COD_{Mn} removal increased dramatically with *in situ* MnO_2. This enhanced coagulation effect was even more apparent at low coagulant dosage. When the dosage of PAS was 2 mg/L, the removal of UV_{254} and COD_{Mn} were 9.2% and 2.5%, respectively. When 10 mg/L of *in situ* MnO_2 was added, the removal of UV_{254} and COD_{Mn} increased to 55.0% and 38.9%, respectively. In contrast, the UV_{254} removal remained unchanged

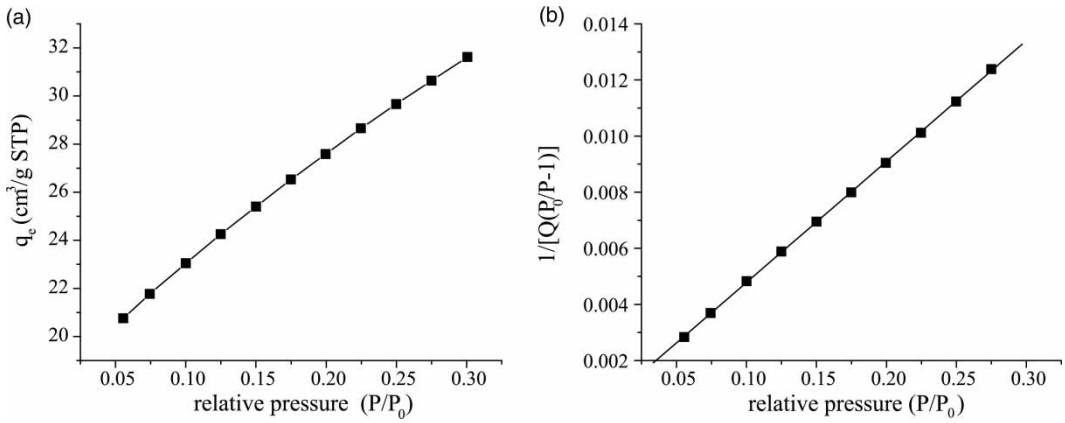

Figure 3 | (a) Adsorption isotherm of N_2 on MnO_2; (b) specific surface area of N_2 on MnO_2.

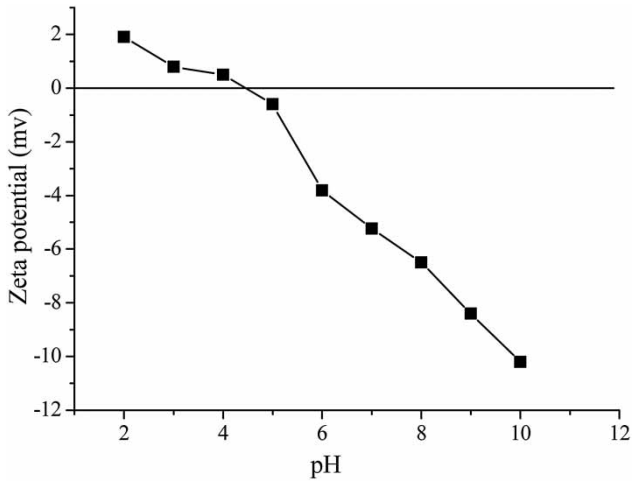

Figure 4 | pH_{ZPC} of the *in situ* MnO_2.

and the COD_{Mn} removal increased to a far lesser extent when commercially available MnO_2 particles were used. The reason for this difference is that *in situ* MnO_2 has strong adsorption capacity at low coagulant dosage. Therefore, adding a certain amount of *in situ* MnO_2 can effectively enhance the removal of organic matter from water. In contrast, commercially available MnO_2 has weak adsorption capacity, and its enhanced coagulation efficacy is not significant.

Effect of pH value on enhanced coagulation

The pH value is an important factor that affects the coagulation efficiency. The pH value can impact both the reaction and the product of coagulant in water, and it also influences the amount of organic matter in water (Xie *et al.* 2012).

As shown in Figures 6(a) and 6(b), at $pH \leq 4.0$, humic acid removal was higher than under alkaline conditions. Specifically, the humic acid removal by UV_{254} method reached 65.9% at $pH \leq 4.0$, whereas the humic acid removal by COD_{Mn} method was 32.2%. In alkaline conditions,

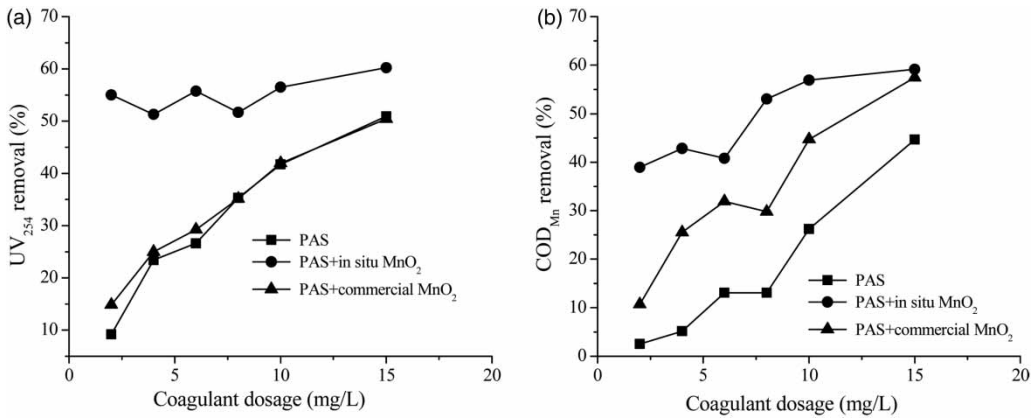

Figure 5 | Effect of the form of MnO_2 on enhanced coagulation.

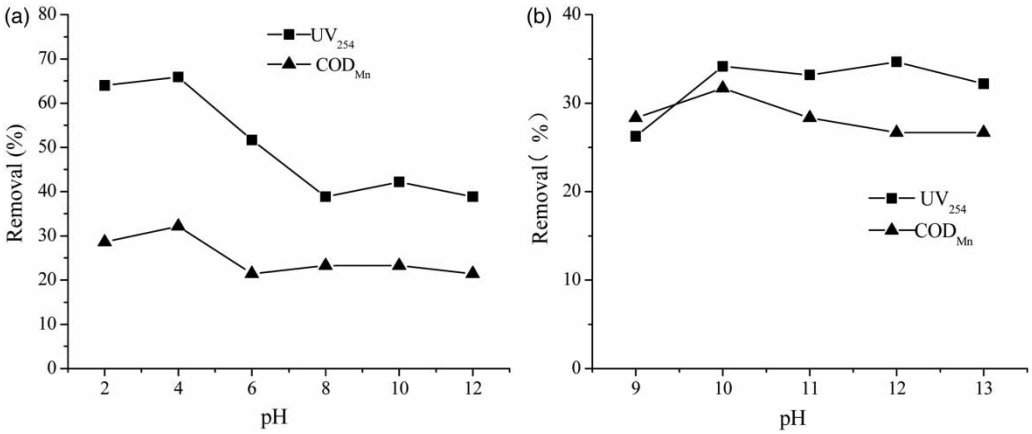

Figure 6 | Effect of pH on enhanced coagulation.

humic acid removal by UV_{254} and COD_{Mn} methods were 40.0% and 25.0%, respectively. This difference can be attributed to the following: at pH = 4.0, PAS hydrolyses in water, forming $Al_8(OH)_{20}^{4+}$. pH 4.0 is close to pH_{ZPC} of *in situ* MnO_2, which causes MnO_2 to aggregate with hydrolysate of PAS through electrostatic attraction. This generates a manganese-dioxide aluminum network that precipitates readily and facilitates the removal of humic acid molecules by adsorption from the aqueous solution. At pH = 2.0, the hydrolysate of PAS is present in the form $[Al(H_2O)_n]^{3+}$ (n = 6–10). The degree of polymerization is less than that for pH = 4.0. At pH > 8.0, PAS takes the forms of $Al(OH)^-$ and $Al(OH)_{26}^{2-}$, and the zeta potential of the *in situ* MnO_2 is less than −8.0 mV; this results in an electrostatic repulsion that negatively impacts adsorption and bridging, so resulting in less of an coagulation enhancement.

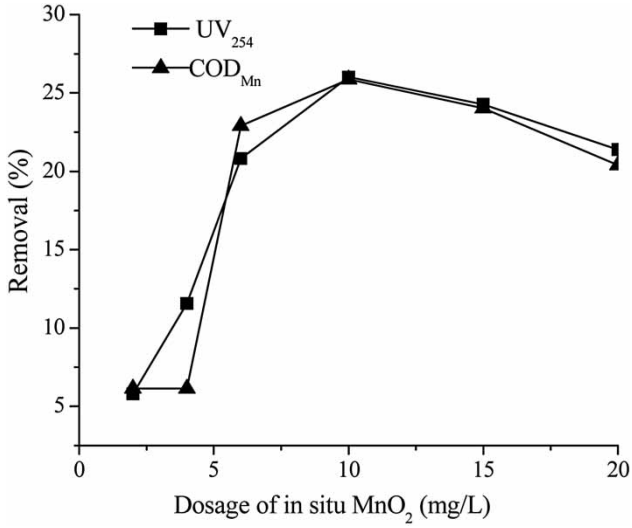

Figure 7 | Effect of *in situ* MnO_2 dosage on enhanced coagulation.

Effect of *in situ* manganese dioxide dosage on the enhanced coagulation

As shown in Figure 7, humic acid removal by UV_{254} and COD_{Mn} methods increased rapidly when the dosage of *in situ* MnO_2 was increased from 2 to 10 mg/L; the UV_{254} removal increased from 5.8 to 26.0%, whereas the COD_{Mn} removal increased from 6.1 to 25.9%. When the dosage of *in situ* MnO_2 was continuously increased from 10 to 20 mg/L, both the UV_{254} and COD_{Mn} removal decreased slightly. Because this study used micro-polluted water, which exhibits low turbidity, this decrease resulted in an increased interparticle distance within the aqueous environment. The addition of *in situ* MnO_2 causes high efficiency of adsorbing organic contaminants and concomitantly increases the probability of interparticle collision, thus way causing large aggregates that precipitate out of the water. Consequently, both the UV_{254} and COD_{Mn} removal increased with increasing dosage of *in situ* MnO_2. With a further increase in the dosage of *in situ* MnO_2, the resultant increase in concentration caused auto-aggregation between MnO_2 species, accordingly reducing its total adsorption capacity. In addition, aggregated MnO_2 clusters reduced the interparticle collision frequency, thereby causing a reduction in coagulation effects.

Effect of the $KMnO_4/MnSO_4$ dosing ratio on enhanced coagulation

The effect of the $KMnO_4/MnSO_4$ dosing ratio on the enhanced coagulation is shown in Figure 8. As the

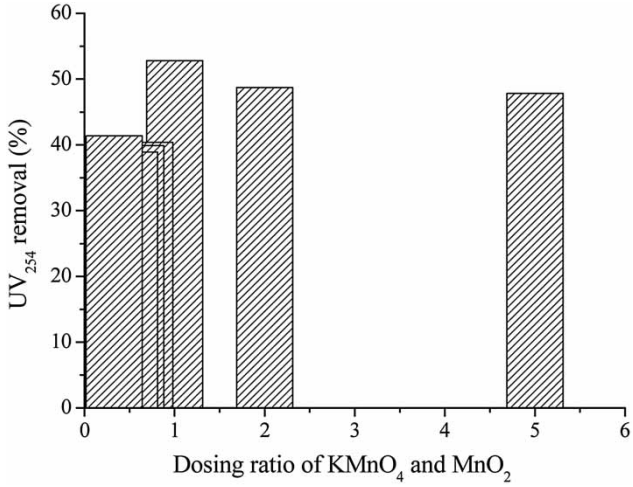

Figure 8 | Effect of $KMnO_4/MnSO_4$ dosing ratio on enhanced coagulation.

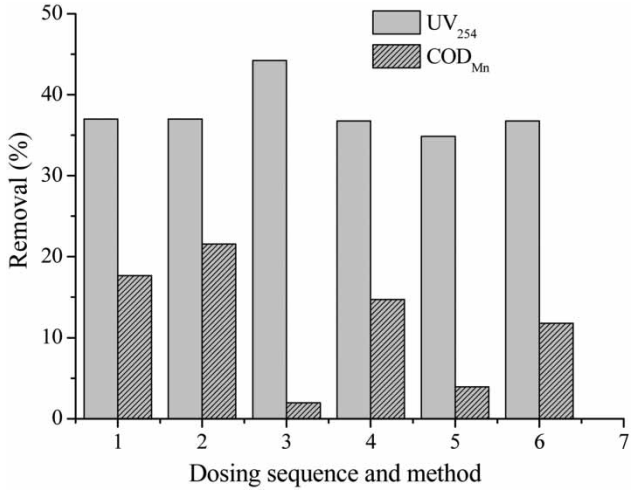

Figure 9 | Effect of dosing sequence and method on enhanced coagulation.

$KMnO_4/MnSO_4$ dosing ratio was decreased from 5 to 0.33, the UV_{254} removal first exhibited an increase, which was followed by a decrease. When the $KMnO_4/MnSO_4$ dosing ratio was greater than 1, the UV_{254} removal increased with decreasing $KMnO_4/MnSO_4$ ratio. This result occurred because as the $KMnO_4/MnSO_4$ dosing ratio became greater than 1, the concentration of $KMnO_4$ was 10 mg/L, whereas that of $MnSO_4$ was less than 10 mg/L. As a result, when the $KMnO_4/MnSO_4$ dosing ratio was greater than 1, $MnSO_4$ became the limiting reagent in the production of *in situ* MnO_2. The concentration of *in situ* MnO_2 increased with decreasing $KMnO_4/MnSO_4$ dosing ratio (increasing $MnSO_4$ concentration), hence increasing the enhanced coagulation effect. When the $KMnO_4/MnSO_4$ dosing ratio was less than 1, the concentration of *in situ* MnO_2 was 10 mg/L, with an excess of $MnSO_4$ in solution. The concentration of excess $MnSO_4$ increased with decreasing $KMnO_4/MnSO_4$ dosing ratio, resulting in an increase of Mn^{2+} species in solution, which hindered the adsorption of small organic molecules, thus reducing the UV_{254} removal efficiency.

Effect of dosing sequence and dosing methods on enhanced coagulation

Six types of dosing method were used: (1) *in situ* MnO_2 (online) + PAS + PAM; (2) PAS + *in situ* MnO_2 (online) + PAM; (3) MnO_2 (commercial source) + PAS + PAM; (4) *in situ* MnO_2 (mixed first then added) + PAS + PAM; (5) PAS + MnO_2 (commercial source) + PAM; and (6) PAS + PAM.

The effect of the dosing sequence and methods on coagulation is shown in Figure 9. The UV_{254} removal was consistent among all methods, with a value of approximately 40%, which indicates that the differences in dosing methods and sequence had little effect on the UV_{254} removal. However, method 2 resulted in the optimal COD_{Mn} removal of 21.6%. In comparison with method 6, the COD_{Mn} removal was double in method 2. The addition of *in situ* MnO_2 resulted in better COD_{Mn} removal compared with commercially available MnO_2. In addition, the removal efficiency was greater when the *in situ* MnO_2 was added after the addition of PAS compared with that when the *in situ* MnO_2 was added before the addition of PAS. This result can be attributed to the fact that *in situ* MnO_2 is not yet aggregated, in contrast with commercially available MnO_2. Therefore, *in situ* MnO_2 possesses a greater adsorption capacity. Furthermore, addition of *in situ* MnO_2 can enhance coagulation through adsorption bridging, which leads to a stronger coagulation effect. Addition of *in situ* MnO_2 after the coagulant facilitates the formation of aggregates of PAS with stronger coagulation efficiency and $[Al(OH)_3]_m$ precipitate, thus enhancing humic acid adsorption in water.

Orthogonal array analysis of the enhanced coagulation parameters

The results of orthogonal test are summarized in Tables 1 and 2. In Table 2, K_i ($i = 1, 2, 3$) is the sum of humic acid removal by UV_{254} and COD_{Mn} methods at the same codified factor I; k_i ($i = 1, 2, 3$) is the average value of humic acid removal at the same codified factor i; R is the difference value between the maximum of k_i and the minimum k_i, $R = \max(k_i) - \min(k_i)$, which can identify the order of significant factors.

Table 1 | A standard L_9 (3^4) matrix

	Factors							
	Codified factors				Numerical values			
Experiments	pH	*In situ* MnO_2 dosage (mg/L)	Slow stirring time (min)	Particulate concentration (mg/L)	pH	*In situ* MnO_2 dosage (mg/L)	Slow stirring time (min)	Particulate concentration (mg/L)
1	1	1	1	1	4	6	20	10
2	1	2	2	2	4	10	30	20
3	1	3	3	3	4	15	40	30
4	2	1	2	3	6	6	30	30
5	2	2	3	1	6	10	40	10
6	2	3	1	2	6	15	20	20
7	3	1	3	2	8	6	40	20
8	3	2	1	3	8	10	20	30
9	3	3	2	1	8	15	30	10

Table 2 | A standard L_9 (3^4) matrix analysis and humic acid removal

		Factors					
		Codified factors				Humic acid removal (%)	
	Experiments	pH	*In situ* MnO_2 dosage (mg/L)	Slow stirring time (min)	Particulate concentration (mg/L)	UV_{254}	COD_{Mn}
	1	1	1	1	1	67.2	63.3
	2	1	2	2	2	71.2	61.2
	3	1	3	3	3	71.2	57.1
	4	2	1	2	3	18.4	20.4
	5	2	2	3	1	22.4	24.5
	6	2	3	1	2	17.6	28.5
	7	3	1	3	2	32.8	44.9
	8	3	2	1	3	31.6	42.8
	9	3	3	2	1	29.6	38.7
Sum of K_i and average of k_i by UV_{254} method	K_1	209.6	118.4	116.4	119.2		
	K_2	58.4	125.2	119.2	121.6		
	K_3	94.0	118.4	126.4	121.6		
	k_1	69.9	39.5	38.8	39.7		
	k_2	19.5	41.7	39.7	40.5		
	k_3	31.3	39.5	42.1	40.5		
	R	50.4	2.3	3.3	0.8		
Sum of K_i and average of k_i by COD_{Mn} method	K_1	181.6	128.5	134.6	126.4		
	K_2	73.4	128.5	120.3	134.6		
	K_3	126.4	124.4	126.4	120.3		
	k_1	60.5	42.8	44.9	42.2		
	k_2	24.5	42.8	40.1	44.9		
	k_3	42.2	41.5	42.2	40.1		
	R	36.1	1.4	4.8	4.8		

It can be found from Table 2 that for the UV_{254} removal, the pH of the water was the greatest contributing factor, followed by the slow stirring time, then the *in situ* MnO_2 dosage, and finally the concentration of particulates. The R value was 50.4 for the pH factor, which is significantly greater than the R values for the factors of *in situ* MnO_2 dosage, slow speed stirring time, and concentration of particulates. This result indicates that pH is the dominant determinant of the UV_{254} removal efficiency. For the COD_{Mn} removal, the pH was also found to be the dominant factor, and the rest of the parameters are ranked in order of decreasing significance as follows: slow stirring time > particulate concentration > manganese dioxide dosage. Comparing the R values for each parameter, the R value for pH factor is high for both UV_{254} and COD_{Mn} removal. Furthermore, at pH = 4, the removal of UV_{254} and COD_{Mn} was far greater than at pH = 6.0 and pH = 8.0. This result is consistent with the results obtained through single-factor analysis. By comparing the K values of the orthogonal test, the following can be deduced: for maximal UV_{254} and COD_{Mn} removal, a pH of 4.0, *in situ* MnO_2 dosage of 10 mg/L, slow stirring time of 20 or 40 min, and particulate concentration at 20 or 30 mg/L should be used.

CONCLUSIONS

In situ MnO_2-enhanced coagulation can significantly improve humic acid removal efficiencies of PAS. At pH = 4, the enhancement of coagulation was most apparent when the dosage of PAS was 2 mg/L and the dosage of *in situ* MnO_2 was 10 mg/L. Humic acid removal by UV_{254} and COD_{Mn} methods increased from 9.2% and 2.5% to 55.0% and 38.9%, respectively, upon the addition of *in situ* MnO_2.

The effect of *in situ* MnO_2 on coagulation enhancement is most affected by pH, whereas the effects of the other parameters rank in order of decreasing significance as follows: slow stirring time > particulate concentration > MnO_2 dosage.

The use of *in situ* MnO_2 as a coagulant additive enhances the coagulation effect of PAS, which can effectively improve the removal of humic acid. The dissolved aluminum and manganese content after treatment met the corresponding water standards, and there was no secondary pollution. This method is easy to use and economically sound. This work provides a scientific basis and reference for the removal of humic acid through enhanced coagulation.

ACKNOWLEDGEMENT

The authors thank the planning project on innovation and entrepreneurship training of China University for financial support.

REFERENCES

Brattebø, H., Ødegaard, H. & Halle, O. 1987 Ion exchange for the removal of humic acids in water treatment. *Water Research* **21** (9), 1045–1052.

Chai, X. L., Hao, Y. X., Liu, G. X., Zhao, X. & Zhao, Y. C. 2013 Spectroscopic studies of the effect of aerobic conditions on the chemical characteristics of humic acid in landfill leachate and its implication for the environment. *Chemosphere* **91** (7), 1058–1063.

El-Rehaili, A. M. & Weber, W. J. 1987 Correlation of humic substance trihalomethane formation potential and adsorption behavior to molecular weight distribution in raw and chemically treated waters. *Water Research* **21** (5), 573–582.

Fan, C. Z., Lu, A. H., Li, Y. & Wang, C. Q. 2010 Pretreatment of actual high-strength phenolic wastewater by manganese oxide method. *Chemical Engineering Journal* **160** (1), 20–26.

Fang, J. P., Zhang, P. Y. & Zeng, G. M. 2008 Research on humic acid adsorption by modified C linoptilolite. *Chinawater & Wastewater* **24** (23), 48–51 (in Chinese).

Fathy, N. A., El-Shafey, S. E., El-Shafey, O. I. & Mohamed, W. S. 2013 Oxidative degradation of RB19 dye by a novel γ-MnO_2/MWCNT nanocomposite catalyst with H_2O_2. *Journal of Environmental Chemical Engineering* **1** (4), 858–864.

Ghernaout, D., Ghernaout, B., Saiba, A., Boucherit, A. & Kellil, A. 2009 Removal of humic acids by continuous electromagnetic treatment followed by electrocoagulation in batch using aluminium electrodes. *Desalination* **239** (1–3), 295–308.

Huang, T. L. 1999 DBPs precursor removal by enhanced coagulation in water purification process. *ACTA Scientiae Circumstantiae* **19** (4), 399–404 (in Chinese).

Kosmulski, M. 2014 The pH dependent surface charging and points of zero charge. VI. Update. *Journal of Colloid and Interface Science* **426** (15), 209–212.

Ladavos, A. K., Katsoulidis, A. P., Iosifidis, A., Triantafyllidis, K. S., Pinnavaia, T. J. & Pomonis, P. J. 2012 The BET equation, the inflection points of N_2 adsorption isotherms and the estimation of specific surface area of porous solids. *Microporous and Mesoporous Materials* **151** (15), 126–133.

Leodopoulos, Ch, Doulia, D., Gimouhopoulos, K. & Triantis, T. M. 2012 Single and simultaneous adsorption of methyl orange and humic acid onto bentonite. *Applied Clay Science* **70** (12), 84–90.

Liang, H. F., Ma, Z. C., Zhang, J. & Hu, Z. J. 2005 Study on the removal of As(III) in water by the in situ manganese dioxide. *Environmental Pollution Control* **27** (3), 168–170 (in Chinese).

McKnight, D. M. & Aiken, G. R. 1998 Sources and age of aquatic humic. In: *Aquatic Humic Substances: Ecology and*

Biogeochemistry (D. O. Hessen & L. J. Tranvik, eds). Ecological studies, **133**, 9–39.

Savaji, K. V., Niitsoo, O. & Couzis, A. 2014 Influence of particle/solid surface zeta potential on particle adsorption kinetics. *Journal of Colloid and Interface Science* **431** (10), 165–175.

Song, H. C. 2012 *Removal of Natural Organic Matter in Water with Modified Ultrafiltration Membrane*. Shanghai JiaoTong University, Shanghai (in Chinese).

Standard Methods for the Examination of Water and Wastewater 1998 20th edn, American Public Health Association/ American Water Works Association/Water Environment Federation. Washington, DC, USA.

Traversa, A., Orazio, V. D., Mezzapesa, G. N., Bonifacio, E., Farrag Senesi, K. N. & Brunetti, G. 2014 Chemical and spectroscopic characteristics of humic acids and dissolved organic matter along two Alfisol profiles. *Chemosphere* **111** (9), 184–194.

Wan, S. L., Ma, M. H., Lv, L., Qian, L. P., Xu, S. Y., Xue, Y. & Ma, Z. Z. 2014 Selective capture of thallium(I) ion from aqueous solutions by amorphous hydrous manganese dioxide. *Chemical Engineering Journal* **239** (3), 200–206.

Wang, W. D., Wang, W., Fan, Q. H., Wang, Y. B., Qiao, Z. X. & Wang, X. C. 2014 Effects of UV radiation on humic acid coagulation characteristics in drinking water treatment processes. *Chemical Engineering Journal* **256** (11), 137–143.

Wu, Y. Y., Zhou, S. Q. & Qin, F. H. 2010 Removal of humic acids by oxidation and coagulation during Fenton treatment. *Environmental Science* **31** (4), 996–1000 (in Chinese).

Xie, J. K., Wang, D. S., Leeuwen, J., Zhao, Y. M., Xing, L. N. & Chow, C. W. K. 2012 pH modeling for maximum dissolved organic matter removal by enhanced coagulation. *Journal of Environmental Sciences* **24** (2), 276–283.

Xu, M., Wang, H. J., Lei, D., Qu, D., Zhai, Y. J. & Wang, Y. L. 2013 Removal of Pb(II) from aqueous solution by hydrous manganese dioxide: adsorption behavior and mechanism. *Journal of Environmental Sciences* **25** (3), 479–486.

Zhang, L. Z. & Ma, J. 2008 The microtopography of manganese dioxide formed in situ and its adsorptive properties for organic micropollutants. *Solid State Science* **10** (2), 148–153.

First received 26 December 2014; accepted in revised form 27 April 2015. Available online 12 May 2015